PCCP

Photoelectron-photofragment coincidence spectroscopy of aromatic carboxylates: benzoate and p-coumarate

SCHOLARONE™
Manuscripts

Journal Name

Photoelectron photofragment coincidence spectroscopy of aromatic carboxylates: benzoate and *p*-coumarate[†]

J. A. Gibbard,[a] E. Castracane,[a] A. I. Krylov[b] and R. E. Continetti[a*]

Photoelectron-photofragment coincidence spectroscopy was used to study the dissociation dynamics of the conjugate bases of benzoic acid and *p*-coumaric acid. Upon photodetachment at $266\,\mathrm{nm}$ ($4.66\,\mathrm{eV}$) both aromatic carboxylates undergo decarboxylation, as well as the formation of stable carboxyl radicals. The key energetics are computed using high-level electronic structure methods. The dissociation dynamics of benzoate were dominated by a two-body DPD channel resulting in $CO_2 + C_6H_5 + e^-$, with a very small amount of stable $C_6H_5CO_2$ showing that the ground state of benzoate is stable and the excited states are dissociative. For *p*-coumarate (*p*-CA$^-$) the dominant channel is photodetachment resulting in a stable radical and a photoelectron with electron kinetic energy (eKE) $< 2\,\mathrm{eV}$. We also observed a minor two-body dissociative photodetachment (DPD) channel resulting in $CO_2 + HOC_6H_4CHCH + e^-$, characterized by eKE $< 0.8\,\mathrm{eV}$. Evidence was also found for a three-body ionic photodissociation channel producing $HOC_6H_5 + HCC^- + CO_2$. The ion beam contained both the phenolate and carboxylate isomers of *p*-CA$^-$, but DPD only occurred from the carboxylate form. For both species DPD is seen from the first and second excited states of the radical, where vibrational excitation is required for decarboxylation from the first excited radical state.

1 Introduction

Light drives many important processes in biology including vision, photosynthesis, and phototaxis. The photocycle is initiated by the response of a chromophore within the photoactive protein to light of a particular wavelength. Structural changes initiate a cascade of transformations in the chromophore upon absorption of a photon, ultimately resulting in a biological response of the organism. One well-studied example is the photoactive yellow protein (PYP), which is responsible for the negative phototaxis exhibited by the Halorjodospira halophila bacteria in response to harmful blue light.[1] The chromophore of PYP is a deprotonated para-coumaric acid anion (*p*-CA$^-$) which is covalently bound to the protein backbone via a cysteine residue and is enveloped in a network of hydrogen bonds. Irradiation with blue light results in *cis-trans* isomerization of *p*-CA$^-$, a first step in the photocycle that ultimately causes the bacterium to move away from the light.[2] The dynamics of simplified model and isolated chromophores are the subject of significant interest, as a first step towards understanding the role of the protein environment and the presence of competing channels to the desired photochemical pathway.[2–6] Previous studies have indicated that internal conversion, intersystem crossing, intramolecular vibrational redistribution, and isomerization can occur.[7–12] However, the dissociation dynamics of *p*-CA$^-$ and other prototypical aromatic carboxylates, such as benzoate, above the carboxylate photodetachment threshold have not been investigated.

When the photodetachment of an anion results in a neutral on a dissociative potential energy surface, fragmentation occurs readily, leading to two or more neutral fragments via a dissociative photodetachment (DPD) process. Although similar channels have been observed in other carboxylates,[13] no work to date has focused on their potential presence in *p*-CA$^-$. Photoelectron-photofragment coincidence (PPC) spectroscopy couples photoelectron spectroscopy and translational spectroscopy to give a kinematically complete picture of DPD.[14] Previously, the high-beam-energy PPC spectrometer, which consists of an electrospray ionization (ESI) source, a hexapole accumulation trap and a linear accelerator (LINAC) to produce fast anion beams, has been used to study the decarboxylation dynamics of the simplest dicarboxylic

[a] Department of Chemistry and Biochemistry, University of California, San Diego, 9500 Gilman Dr, La Jolla, CA, 92093-0340

[b] Department of Chemistry, University of Southern California, Los Angeles, CA, 90089-0482

* E-mail: rcontinetti@ucsd.edu

† Electronic Supplementary Information (ESI) available.

acid, the oxalate monoanion.[15] Benzoate and p-CA$^-$ are both aromatic carboxylate anions and have been the focus of previous photoelectron spectroscopy studies.[2–6,16] The structures of benzoic and p-coumaric acid are shown in the supplementary information (SI) in Figure S1. The present work reports a high-beam-energy PPC spectroscopy study that investigates the DPD dynamics of benzoate and p-CA$^-$ in a kinematically complete manner for the first time. The experimental measurements are supplemented by high-level electronic structure calculations.

The photodetachment and DPD dynamics of benzoate have previously been studied using photoelectron spectroscopy and the detection of neutral fragments, respectively.[16,17] Wang and coworkers have recorded the photoelectron spectra of 18 K, 70 K and 300 K benzoate at 266 nm (4.66 eV) and 193 nm (6.42 eV).[16] The spectra showed five distinct features that were assigned to electronic states; a broad, low intensity feature was assigned to the ground X state of the neutral, A and B bands were assigned to photodetachment of the carboxylate group, and C and D bands were assigned to photodetachment of electrons from the benzene $\pi-$system. The broad X feature was attributed to the large change in OCO bond angles upon photodetachment ($\approx 19°$). Vibrational structure was observed at all temperatures in the A and B bands, attributed to excitation of OCO bending modes and suggesting a neutral with a lifetime longer than the vibrational period of the radical. Calculations indicated a planar anion and radical structure, where the neutral has a shorter $H_5C_6-CO_2$ bond length and a smaller OCO bond angle than in the anion. Jouvet and coworkers studied the DPD of benzoate at 315 nm and 225 nm using cold ion photofragment spectroscopy.[17] DPD was the dominant channel, but a small amount of stable benzoate radical was also observed. No ionic photodissociation channels were reported. It was assumed that the photofragments resulting from DPD were $C_6H_5 + CO_2 + e^-$, but neither the fragment mass spectrum nor the kinetic energy release (KER) spectrum of the dissociation were directly measured. Calculations indicated that the DPD dissociation asymptote was 3.3 eV above the energetic ground state of the anion, however the EA of the phenyl radical was significantly underestimated using the same theoretical approach (0.5 eV vs 1.1 eV).[17,18]

There are two acidic protons in p-coumaric acid, such that two deprotomers of p-CA$^-$ exist, known as the phenolate and carboxylate isomers. The phenolate form of p-CA$^-$ resembles the chromophore of PYP most closely. The phenolate isomer has two resonance stabilized forms that effectively delocalize the charge across the entire molecule, resulting in greater stability in the gas phase. However, the carboxylate is stabilized more in protic and polar solvents. The resonance forms of both isomers are shown in Figure S2 in the SI. Oomens and coworkers aimed to determine the proportion of tautomers of p-CA$^-$ produced during ESI.[19] IR spectroscopy of gas-phase p-CA$^-$ determined that the phenolate isomer can be formed in the gas phase via ESI when a dry acetonitrile solvent is used, but the addition of any protic solvent increases the proportion of the carboxylate isomer present.[19] Figure 1 shows essential details of the electronic structure of the low-lying radical states produced by photodetachment of benzoate and the phenolate
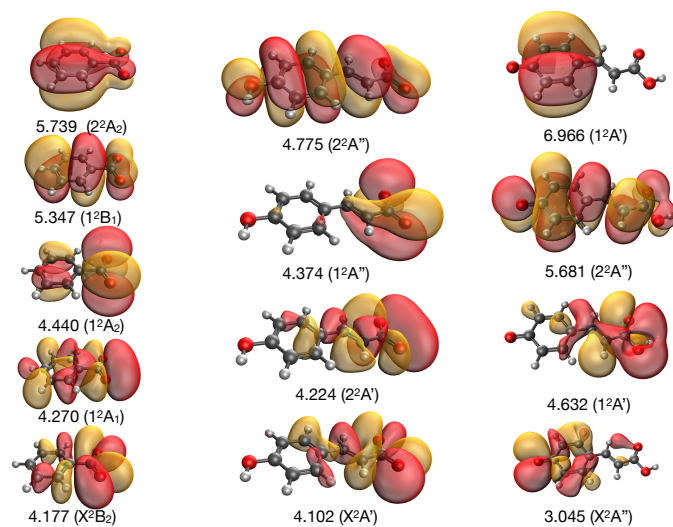
Fig. 1 Ionization energies (eV) and Dyson orbitals produced via a one-electron photodetachment of benzoate (left), the carboxylate form of p-CA$^-$ (center), and the phenolate of p-CA$^-$ (right), calculated using EOM-IP-CCSD/aug-cc-pVTZ.

and carboxylate forms of deprotonated p-coumaric acid. Closed shell anionic chromophores, such as benzoate, the phenolate and carboxylate forms of p-CA$^-$, and green fluorescent protein (GFP) model chromophores have relatively large detachment energies but, with the exception of the GFP chromophore, do not support bound excited states.[20–24] However, electrostatic interactions with a polar solvent or a protein environment stabilize the anionic states and increase the detachment energies significantly, making anionic excited states bound with respect to electron detachment.[20,21] In addition, these anions feature low-lying repulsive states that can result in photodissociation.[25]

A number of studies have probed the dynamics of the isolated PYP chromophore using photoelectron spectroscopy. Zewail and coworkers studied the methylated phenolate tautomer ($^-OC_6H_4CHCHCOCH_3$) using time-resolved photoelectron spectroscopy.[3] The first observed step in the photocycle of PYP is a twisting of the double bond, which is readily observed in the isolated chromophore on a timescale of < 1 ps. From this work the role of the protein environment in PYP was determined to be funneling the excited, twisted state of the anion into a conical intersection leading to cis-products, and suppressing electron detachment and radical formation. Fielding and coworkers recorded the photoelectron spectra of the deprotonated phenolate form of the anion, along with the meta- and ortho-substituted variants, in the $364 - 315$ nm ($3.41 - 3.94$ eV) range.[2,4–6] They reported a broad feature at low electron binding energy (eBE where eBE= $h\nu-$ eKE) and a sharp feature at high eBE.[2] By considering the spectra at multiple wavelengths, they attributed the feature at low eBE to a direct photodetachment channel close to the calculated vertical detachment energy (VDE) and the high eBE feature to an indirect photodetachment process as the eBE shifted with wavelength. This high eBE feature was attributed to indirect photodetachment from the $1^1\pi\pi^*$ state and thermionic emission from S_0. Calculations in

the Fielding study indicated that the VDE for the phenolate form of the anion was $2.7 - 3$ eV and $4.7 - 4.9$ eV for the carboxylate anion, such that only the phenolate anion was determined to be accessible at the wavelength range they used. They attributed the intensity of the indirect photodetachment channel, especially at 364 nm (3.41 eV), to the large oscillator strengths at the near-resonant photon energy and vertical excitation energies of the $1^1\pi\pi^*$ states. They suggested that the protein restricts torsional motion in the electronic ground state and impedes radical formation by electron emission. Theoretical work has further indicated that the protein environment or the presence of solvent stabilizes the anionic states of the chromophore and increases the VDE,[25] as has been observed experimentally for the model chromophore of GFP.[26] Fielding and co-workers also investigated the role of substitution at the coumaric acid group and the effect of restricting *cis-trans* isomerization using photoelectron spectroscopy. This was achieved by studying an ethane-bridged version of coumaric acid to examine the effect on the competition between various electronic relaxation processes and electron emission.[4,5] No photoelectron spectrum of the carboxylate form of *p*-CA$^-$ has been reported.

Numerous studies have probed the spectroscopy of *p*-CA$^-$ and various derivatives by recording neutral products, using an electrostatic ion storage ring, absorption spectroscopy, daughter mass analysis and time of flight spectroscopy.[7–11] Nielsen and coworkers initially reported the gas phase and solution phase absorption spectrum of *p*-CA$^-$.[7] The gas phase spectrum for *p*-CA$^-$ peaked at 430 nm (2.88 eV), whereas the maximum absorption for PYP was found to be 446 nm (2.78 eV). Additionally the absorption maximum of a neutral solution of *p*-CA was 285 nm (4.35 eV), shifting to 336 nm (3.69 eV) at pH $= 11$. These results were interpreted to indicate that the absorption spectrum of PYP was largely determined by the chromophore itself, but that the protein environment played a significant role through hydrogen bonding, charge distribution and geometric strain. Andersen and coworkers studied the photodissociation dynamics of *p*-CA$^-$ over a range of timescales, from several nanoseconds to seconds, using a merged beam setup with an electrostatic ion storage ring.[8] Daughter ion fragments of mass 119 ± 2 a.m.u. were observed, attributed to $HOC_6H_4CHCH^-$ and neutral CO_2. The data revealed a fast and slow channel assigned to electron emission and statistical fragmentation. One interpretation presented was that absorption near 400 nm produced an excited, bound anionic state leading to a rearrangement of the nuclear geometry. Autodetachment of this excited state resonance then led onto the neutral potential energy surface. The other pathway involved internal conversion back to the anion ground state, yielding a vibrationally excited parent anion followed by statistical fragmentation. The exact admixture of isomers present in the ion beam was not known, but the carboxylate was expected to dominate as the ions were produced by ESI using a protic solvent.

Bieske and coworkers used tandem ion mobility mass spectroscopy and laser excitation to study the photophysics of different isomers of *p*-CA.[12] ESI formed the *E* phenolate deprotomer and both the *E* and *Z* carboxylate deprotomers.

The *E* isomer of the phenolate form of *p*-CA$^-$ exhibited photodetachment over the range of $350 - 460$ nm ($3.54 - 2.70$ eV) . Photoexcitation of either carboxylate isomer of *p*-CA$^-$ over $290 - 360$ nm ($4.28 - 3.44$ eV) was found to result in isomerization. The *E* isomer was reported to undergo an enol-keto phototautomerism followed by statistical rearrangement to form the phenolate form of *p*-CA$^-$, whereas the *Z* isomer was reported to undergo photoisomerization to form the E carboxylate deprotomer in competition with photodetachment.

Previously PPC spectroscopy has been used to study the decarboxylation dynamics of a number of other carboxylates including the oxalate monoanion, formate, and acetate.[13,27,28] By recording the photofragments in coincidence with the photoelectron on an event by event basis, PPC spectroscopy provides a more complete picture of decarboxylation than the other methods previously used to study aromatic carboxylates. In all previous PPC spectroscopy studies of carboxylates the dominant dissociation channel was two-body DPD resulting in $RCO_2^- \xrightarrow{h\nu} R + CO_2 + e^-$. This manuscript describes a PPC spectroscopy study of benzoate and *p*-CA$^-$, marking the first time the decarboxylation dynamics of aromatic carboxylates have been studied by collecting all the fragments in coincidence. No previous study has determined the products of DPD, recorded the KER spectrum or directly characterized the nature of the electronic states in benzoate or the DPD dynamics of p-CA$^-$.

2 Structure and Energetics

Figure 2 shows the energy diagram for benzoate and *p*-CA$^-$. The energetics of the anion states, the corresponding radical states and energetically accessible ionic photodissociation and DPD channels are shown relative to the anion ground state. The energies given for the radicals produced by photodetachment of benzoate are the experimental adiabatic detachment energies (ADE) for the *X*, *A*, *B* and *C* states and the threshold detachment energy (TDE) of the *D* state, reported by Wang and coworkers.[16] The ADEs from the anion ground state to the radical electronic states are reported to be 3.59 eV, 3.95 eV, 4.19 eV and 5.14 eV for the *X*, *A*, *B* and *C* states. In the right frame of Figure 2 energetics for *p*-CA$^-$ are shown. Krylov and coworkers have previously studied the electronic structure of the two tautomers of *p*-CA$^-$ [25], reporting optimized geometries and energetics for the anions and the corresponding neutrals, resulting in the VDEs shown in the right hand panel of Figure 2. The VDEs of the carboxylate and phenolate anion are calculated to be 4.10 eV and 3.04 eV respectively, with the phenolate tautomer being more stable by 0.43 eV. Two and three radical states are energetically accessible with a 266 nm (4.66 eV) photon from the phenolate and carboxylate anion ground state respectively. Neither tautomer supports electronically bound excited anion states, such that the lowest valence excitations are anionic resonances embedded in the detachment continuum.[25]

Dissociation asymptotes for benzoate and *p*-CA$^-$ were calculated in the present work using high-level electronic structure methods, as described in section 3. Two photodissociation channels and one DPD channel are energetically accessible from the benzoate anion ground
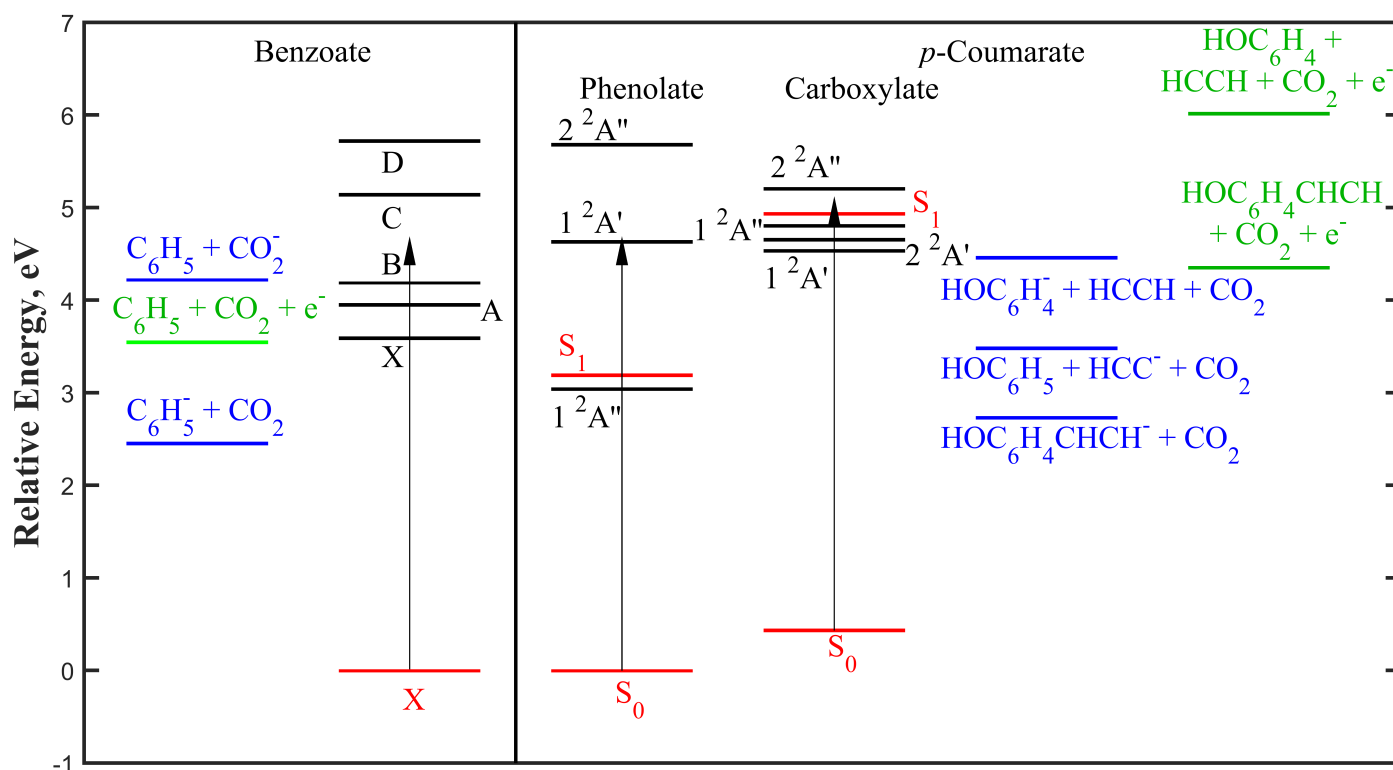
Fig. 2 The relative energetics of the anion (red) and neutral (black) states and the photodissociation (blue) and DPD (green) dissociation asymptotes of benzoate and the tautomers of p-CA$^-$, plotted relative to the ground state of benzoate and the phenolate form of p-CA$^-$.[16,17,25]

state with a 266 nm (4.66 eV) photon, with the X, A and B radical states higher in energy than the DPD product channel ($C_6H_5 + CO_2 + e^-$). At 4.66 eV photodissociation and DPD is energetically accessible from both the phenolate and carboxylate ground state of p-CA$^-$, but CO_2 loss is only facile from the carboxylate. The energetically accessible $1^2A''$ and $2^2A'$ electronic states of the carboxyl form of p-CA lie higher in energy than $HOC_6H_4CHCH + CO_2 + e^-$, whereas $1^2A'$ is approximately the same energy as that lowest DPD asymptote. Table 1 summarizes all the computed energetics of the dissociation asymptotes for both benzoate and p-CA$^-$, reported relative to the anion ground state. From these energetics the EA of C_6H_5 is given as 1.088 eV, in excellent agreement with the previously reported experimental value of 1.09 eV.[18]

3 Experimental and Theoretical Methods

The high-beam-energy PPC spectrometer for heavy and complex ions is shown in Figure 3 and has been described in detail elsewhere.[15] Briefly, the anions are produced via ESI of a 0.2 mmol solution of p-coumaric acid in 1 : 9 mixture of H_2O/CH_3OH or a 2.8 mmol solution of benzoic acid in 1 : 4 mixture of H_2O/CH_3OH and are subsequently desolvated in a heated capillary. Anions are collisionally thermalized to room temperature via collisions with a 298 K He buffer gas in a hexapole accumulation trap. A dense packet of ions is accelerated out of the trap and temporally and spatially compressed to maximize the anion density in the LINAC. The 10-stage LINAC accelerates anions of the correct mass to 11 keV, before the anions

are focused into the detector region. Anions are photodetached with the fourth harmonic (266 nm, 4.66 eV) of a Nd:YAG laser (Ekspla PL2210, pulse width of 27 ps, repetition rate of 50Hz and power density in the interaction region of 3.7 GW cm^{-2}). The photoelectrons are collected perpendicular to the ion beam axis on a time and position sensitive detector. From the x, y position of impact and time of arrival (velocity in the z-direction) of the photoelectron, the angle of recoil and electron kinetic energy (eKE) is determined. The time of arrival measurement induces the largest uncertainty, so only photoelectrons with a narrow distribution of arrival times are included. The final photoelectron spectrum is also corrected using the detector acceptance function that arises from accepting only photoelectrons with minimal z-velocity components.[29] Resulting neutrals, whether fragments or radicals, are detected on a time and position sensitive neutral detector that can record the arrival time and position of up to three neutral fragments in coincidence. Stable radicals will arrive at the detector at the same time as the parent anions and with a spatial profile determined by the laser interaction volume. In contrast, fragments formed via dissociation recoil from the center-of-mass velocity arriving as temporal 'wings' in the time-of-flight spectrum and with a broad distribution of arrival positions across the detector. From this temporal and spatial data the KER of any pairs or triples of fragments formed in the same dissociation event can be extracted,[30] yielding KER and fragment mass spectra. PPC spectroscopy is a coincidence technique and a 2D histogram of N(eKE, KER) for photoelectrons and neutrals is reported as the PPC spectrum, showing the partitioning of kinetic energy in DPD
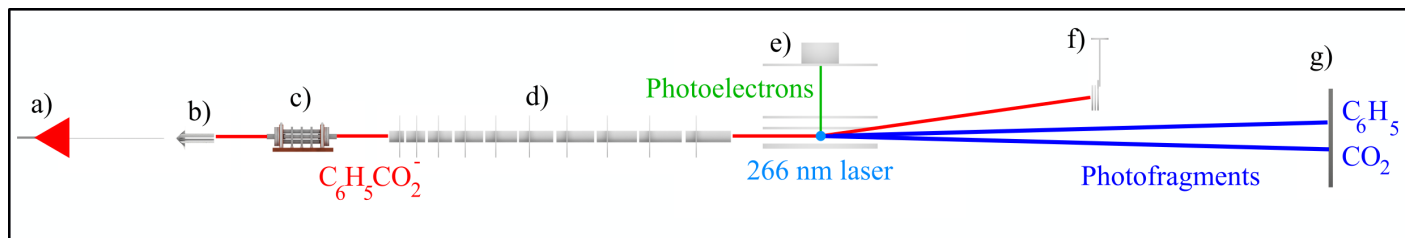
Fig. 3 Schematic of the high-beam-energy PPC spectrometer depicting the a) ESI source, b) octopole ion guide, c) hexapole accumulation trap, d) LINAC, e) electron detector, f) undetached ion deflector and g) neutral detector. The laser intersects the ion beam perpendicular to the plane of the page. A DPD event is shown schematically.

Species	Relative energy, eV
p-CA$^-$ (Phenolate)	0
p-CA$^-$ (Carboxylate)	0.433
$HOC_6H_4CHCH^- + CO_2$	2.730
$HOC_6H_5 + HCC^- + CO_2$	3.481
$HOC_6H_4CHCH + CO_2 + e^-$	4.351
$HOC_6H_4^- + HCCH + CO_2$	4.458
$HOC_6H_4 + HCCH + CO_2 + e^-$	6.015
$C_6H_5CO_2^-$	0
$C_6H_5^- + CO_2$	2.458
$C_6H_5 + CO_2 + e^-$	3.546
$C_6H_5 + CO_2^-$	4.215

Table 1 The relative energetics of the dissociation asymptote of p-CA$^-$ and benzoate with respect to the anion ground state. All values were calculated using CCSD(T)/aug-cc-pVTZ, see text for details. All energies include zero point energy.

events for a given anion. The ion intensity is monitored in real time, by deflecting the unphotodetached ions out of the neutral beam path, after the interaction region, and monitoring them on an ion detector.

Structures and vibrational frequencies of all species except phenyl radical were computed using second-order Møller-Plesset perturbation theory (MP2) with the resolution-of-identity approximation RI-MP2. Due to strong spin-contamination of the Hartree-Fock solution, MP2 yields poor structure for phenyl, leading to large errors in energetics. Therefore, we used B3LYP to compute structures and frequencies of phenyl. Reaction energies were computed using the CCSD(T) method (coupled-cluster with single and double excitations and perturbative account of triples).

For all open-shell species, restricted open-shell Hartree-Fock references were used. Detachment energies and Dyson orbitals (shown in Fig. 1) were computed using EOM-IP-CCSD (equation-of-motion coupled-cluster method for ionization potentials). The calculated VDEs (Figure 1) are higher in energy than the previously reported ADEs for benzoate (Figure 2) due to the expected differences between ADE and VDE, plus the tendency of EOM-IP-CCSD to overestimate energy differences. The aug-cc-pVTZ basis was used in all calculations; core electrons were frozen. Coupled-cluster and EOM-CC calculations were carried out using single-precision execution. [31] All calculations were carried out using the Q-Chem electronic structure program. [32] All Cartesian geometries and relevant energies are given in the SI.

4 Results

We report PPC spectroscopy measurements for benzoate and p-CA$^-$ at a photon energy of 4.66 eV, and present the eKE, KER, PPC and E_{TOT} spectra for both anions, characterizing the observed photodetachment and DPD channels. The total photoelectron spectra can be resolved into stable and dissociative components allowing us to determine the nature of the radical electronic states from the eKE spectra. The KER spectra determine the repulsive character of the dissociative states. We also report kinematically complete PPC spectra that measure the projection of the anionic wavefunction onto the dissociative potential energy surface. Finally the total energy spectra (E_{TOT} = eKE + KER) allow us to determine the presence of different product channels by comparison to calculated KE_{max}, and extract information about the internal energy distribution for both the parent anions and the products.

4.1 Photoelectron spectra

Photodetachment of benzoate results in detection of photoelectrons in coincidence with a stable radical or two neutral fragments, indicating the presence of direct photodetachment and DPD channels, respectively. The total, stable and dissociative spectra can be distinguished in the PPC spectroscopy measurement, and are shown in Figure 4a, which is also annotated at the eKEs corresponding to the previously reported ADEs for photodetachment to the X, A and B radical states as well as an approximate assignment of TDE, that in this case is equal to the ADE for the X state. [16] The TDE is extracted from the onset of photoelectron signal, regardless of the resulting radical electronic state. It is used here as the spectral features
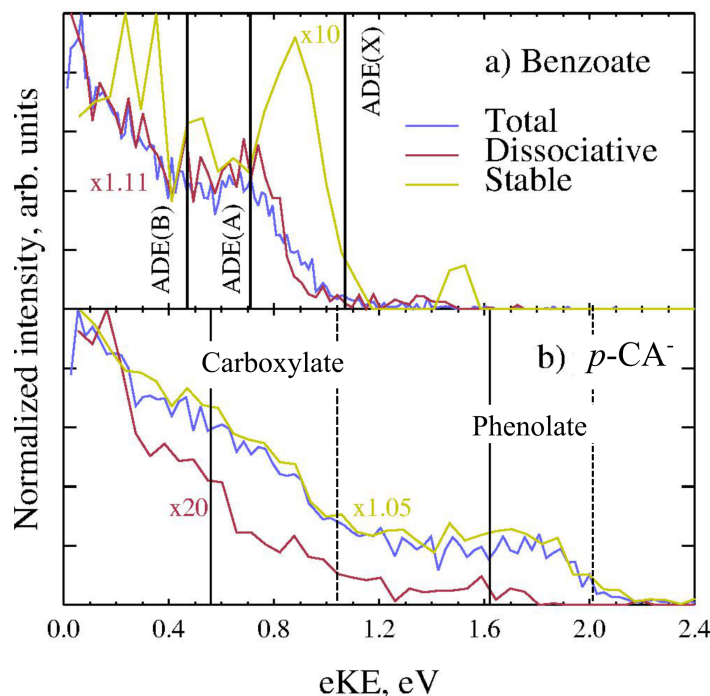
Fig. 4 The total, stable and dissociative eKE spectra of a) benzoate and b) p-CA$^-$ recorded at 266 nm (4.66 eV). The previously reported ADEs for photodetachment of benzoate to the X, A and B radical states are shown in solid black lines in a) and the TDE coincides with ADE(X). [16] In b) the previously calculated VDEs for photodetachment of the carboxylate and phenolate forms of p-CA$^-$ to the corresponding radicals are shown with solid lines and the TDEs for p-CA$^-$ are depicted with dashed lines. [25]

attributed to photodetachment to different radical electronic states overlap significantly. The total photoelectron spectrum of benzoate at 4.66 eV is shown in blue, with the dissociative and stable spectra shown in red and yellow, respectively. The onset of the total photoelectron spectrum, the clear feature centered at eKE = 0.63 eV and the weak rise in signal at eKE = 0.55 eV are attributable to photodetachment to the X, A and B states of the radical, respectively. The total and dissociative spectra are very similar, indicating that a dissociative channel dominates the photodetachment dynamics, with 90% of events resulting in two neutral fragments. The stable photoelectron spectrum has been multiplied by a factor of 10 to aid comparison. It has a different shape to the total or dissociative photoelectron spectra, with a larger proportion of the electrons having eKE > 0.8 eV. However, it is noisy owing to the small branching ratio of photodetachment compared to DPD, and contaminated by contributions from DPD channels where only one of the two neutral fragments are detected at lower eKE. By comparison to the photoelectron spectrum reported by Wang and coworkers, [16] this high eKE onset is attributable to photodetachment to the X state of the radical, and suggests that the X state radical is stable. The energetics in Table 1 indicate that the X state is higher in energy than the DPD asymptote, suggesting that the radical ground state is metastable or long-lived on the timescale of the flight time from the interaction region to the neutral detector ($\approx 10\ \mu$s). The broad X state feature is consistent with a large

geometry change upon photodetachment inducing an extended vibrational progression in the CO_2 bending mode, as reported by Wang and coworkers at an anion temperature of 18 K. [16] However, with the reduced resolution (2% [16] vs 5% [15]) and 300 K temperature of the anions in the present measurement, the vibrational progression is not resolved here. In addition, the high intensity feature observed at eKE = 0 eV is attributable to spurious photoelectrons produced via scattered 4.66 eV photons. The dissociative photoelectron spectrum in Figure 4a shows a small increase in signal in the region of the A and B electronic states (0.5 − 0.75 eV) relative to the total photoelectron spectrum, which is also dominated by dissociative events due to the large DPD branching ratio. This is consistent with DPD occurring via the A and B states.

Photodetachment of coumarate also results in production of both stable radicals and dissociative neutral products. Figure 4b shows the total, stable and dissociative photoelectron spectra of p-CA$^-$ recorded at 4.66 eV and annotated with the calculated VDEs of the phenolate and carboxylate forms of p-CA$^-$ to the corresponding radical ground states as well as the empirical TDE at eKE = 2.06 eV. [25] The total, stable and dissociative photoelectron spectra are shown in blue, yellow, and red respectively. Overall, three distinct regions are observed in the photoelectron spectra: a low eKE feature peaking at eKE = 0.05 eV most intense in the dissociative spectrum, a second broad feature between eKE = 0.3 − 1.0 eV with more intensity in the stable spectrum, and a high energy peak with a long tail centered at eKE = 1.7 eV and extending to eKE = 2 eV where only the stable spectrum has any intensity. As opposed to benzoate, where DPD was dominant, in this case the total and stable spectra are nearly identical, as just 5% of events record a photoelectron in coincidence with two neutral fragments.

The coumarate spectra are consistent with the presence of both the phenolate and carboxylate forms of p-CA$^-$, as expected for an ESI source using a protic solution of p-coumaric acid. [19] From the energetics in Figure 2 five neutral states and two anion resonances (the S_1 states) are energetically accessible from the ground state of the phenolate and carboxylate form of p-CA$^-$. Individual states are not resolved in the photoelectron spectra reported here, as the spectral features are broadened by rotational or vibrational excitation consistent with an anion temperature of 300 K. [15] The high eKE onset of the stable spectrum is similar to the previously reported VDE for the phenolate anion, [2] and the stable spectrum is more intense at the calculated VDE for the carboxylate anion, [25] suggesting that stable phenolate and carboxylate forms of p-CA are observed. The dissociative spectra is the most intense at eKE < 0.3 eV, suggesting the presence of at least one repulsive potential energy surface leading to DPD. Two of the carboxyl states in Figure 2 are higher in energy than the DPD asymptote. In the Fielding study an indirect autodetachment pathway was also observed for the phenolate anions at very low eKE, suggesting the presence of a low eKE stable channel. [2] The oscillator strength is far larger for this transition in the phenolate than the carboxylate. However, it is possible that this anionic resonance will not be populated at the higher photon energy used in this study. Finally, as observed
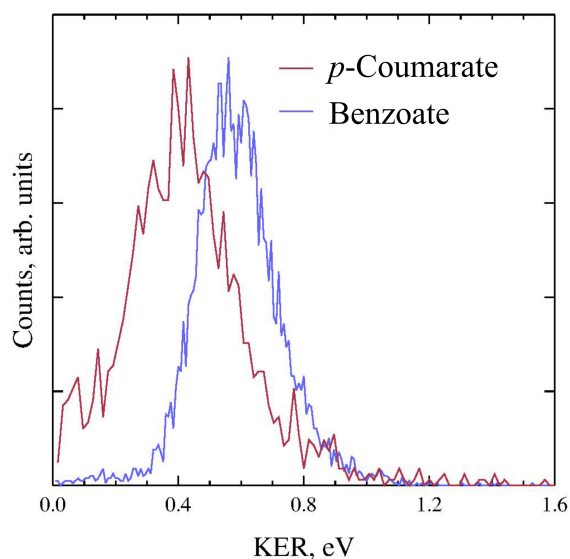
Fig. 5 The KER spectra recorded at 266 nm (4.66 eV) for decarboxylation of benzoate and p-CA$^-$ via two-body DPD.

for benzoate, spurious low eKE electrons can be detected from scattering of 4.66 eV photons with the apparatus. Therefore the lowest eKE feature in the total photoelectron spectra is likely to be a combination of the dissociative carboxylate state leading to DPD, autodetachment of the phenolate form and spurious electrons.

4.2 Kinetic energy release spectra

As noted above, the photodetachment of both benzoate and p-CA$^-$ leads to a branching between the production of stable radicals and DPD producing two momentum-matched neutral fragments detected in coincidence with a photoelectron. The observed partitioning of momentum in both systems is consistent with two-body decarboxylation. The photofragment mass spectra are shown in Figures S3 and S4 in the SI for benzoate and p-CA$^-$, respectively. In the case of benzoate the mass spectrum peaks at 77 and 44 a.m.u. as expected for DPD-decarboxylation producing $C_6H_5 + CO_2 + e^-$. Similar to other PPC spectroscopy studies of the dissociation dynamics of carboxyl radicals, the two-body DPD channel is decarboxylation driven by the thermodynamic stability of CO_2, e.g. $RCO_2^- \longrightarrow R + CO_2 + e^-$.[13] This is also consistent with the previous report of Jouvet and coworkers concerning the DPD of benzoate, although they did not measure the photofragment mass distribution.[17] In the case of p-CA$^-$ the spectrum is broader, consistent with an asymmetric breakup into a light and heavy fragment, with significant intensity out to mass 44 a.m.u. and 119 a.m.u. as expected for the lowest energy dissociation channel yielding $CO_2 + HOC_6H_4CHCH + e^-$. This asymmetric breakup provides strong evidence for the carboxylate form of p-CA$^-$ in the molecular beam.[25] As further discussed in the SI, the p-CA$^-$ photofragment mass spectrum actually peaks $\approx$ 52 and $\approx$ 111 a.m.u., which may be evidence for the charge-symmetric three-body photodissociation channel

producing $HOC_6H_5 + HCC^- + CO_2$. At the relatively low laser power, and low photodetachment cross sections compared to halide anions, the present experiments are not ideal for studying the two low-lying one-photon three-body ionic photodissociation channels shown in Figure 2, as ionic products cannot be detected, so these pathways will not be considered further. The momentum partitioning in the photofragment mass spectra allowed the KER distributions for the two-body decarboxylation DPD for both benzoate and p-CA$^-$ to be determined.

Figure 5 shows the KER spectra for benzoate and p-CA$^-$ recorded at a photon energy of 4.66 eV for two-body DPD resulting in $CO_2 + C_6H_5 + e^-$ and $CO_2 + HOC_6H_4CHCH + e^-$ fragments, respectively. Both KER spectra consist of a single structureless feature. The benzoate KER spectrum peaks at 0.6 eV and extends to 0.95 eV, whereas the p-CA$^-$ KER spectrum peaks at 0.45 eV and extends to 0.7 eV. The peak KER is lower for p-CA$^-$ than for benzoate, and both are similar to the peak KER for the decarboxylation of other carboxylates $(0.4 - 0.7$ eV$)$.[13] The shift to lower KER for p-CA$^-$ indicates either that the dissociative potential energy surface is less repulsive than for benzoate, or that more energy is partitioned to the greater number of internal degrees of freedom in the products of DPD of p-CA$^-$. In the case of benzoate, Figure 2 shows the energy difference between the A and B radical electronic states and the $C_6H_5 + CO_2 + e^-$ DPD asymptote to be 0.40 and 0.64 eV respectively. This energy difference is a theoretical estimate of the KER for DPD via a specific radical state, assuming that the transient neutral and the products are in the rovibrational ground state. The peak KER of the experimental spectrum is between 0.40 and 0.64 eV, suggesting dissociation from both excited states. For p-CA$^-$, the KER spectrum is shifted to higher energies than expected from the calculations, which predict a peak KER between 0.31 and 0.46 eV, assuming DPD from both of the energetically accessible radical states of the carboxyl isomer. It may be that a vertical transition results in a radical far from the equilibrium geometry of the excited radical states and therefore a larger than expected KER.

4.3 Photoelectron-photofragment coincidence spectra

Figure 6a is the PPC spectrum of benzoate at 4.66 eV, for two-body DPD resulting in $CO_2 + C_6H_5 + e^-$. DPD is observed to occur via the A and B states of the radical, indicating that these states are dissociative in character. More intensity is seen at the lower eKEs, characteristic of the B state. From table 1, the energy difference between the anion ground state and the DPD dissociation asymptote is 3.55 eV, indicating that the maximum kinetic energy $KE_{max} = 1.11$ eV is available to partition between the photoelectron and photofragments. The calculated KE_{max} is on the high energy side of the most intense portion of the PPC spectrum, attributed to DPD via the radical B state. The feature attributed to DPD via the radical A state is shifted to higher total energy than the calculated KE_{max}, indicating that DPD is promoted by vibrational excitation for A state radicals and occurs primarily for the hottest anions in the ion beam, where more total energy is available for partitioning to the fragments. The PPC
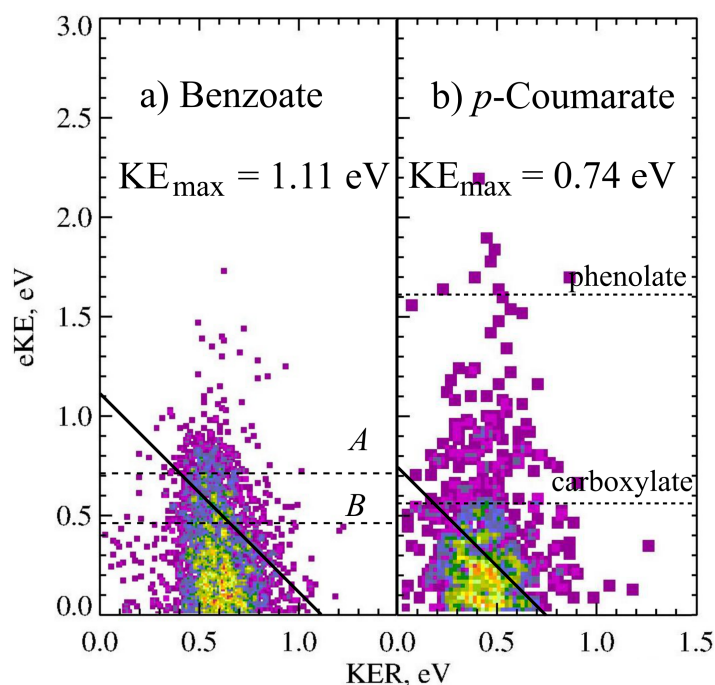
Fig. 6 The PPC spectra for decarboxylation of benzoate and p-CA$^-$ recorded at 266 nm (4.66 eV). The calculated KE$_{max}$ are depicted by the solid diagonal lines. The ADEs for photodetachment of benzoate to the A and B radical states and VDEs of the carboxylate or phenolate p-CA$^-$ to the corresponding radicals are shown in the dashed horizontal lines.

spectrum appears as a single curved feature, due to the overlap of two features resulting from photodetachment to two distinct electronic states. Both states are repulsive in character and result in the same products. However, each state has distinct Franck-Condon factors from the anion ground state, as a result of the differing topography of each repulsive neutral potential energy surface, and is therefore accessed by different anion geometries, resulting in different shapes in the PPC spectrum. It is expected that the vibrational motion in the radical is predominantly in CO_2 localized modes, due to the large change in OCO bond angle following photodetachment.[16]

Figure 6b is the PPC spectra of p-CA$^-$ at 4.66 eV for a two-body DPD channel resulting in $CO_2 + HOC_6H_4CHCH + e^-$. The VDE of the carboxylate form of p-CA$^-$, shown in Figure 6b, is much closer to the onset of the feature in the PPC spectrum than the VDE of the phenolate form. A broad feature is seen in the PPC spectrum with maximum intensity at (eKE, KER)$=(0.3 \text{ eV}, 0.5 \text{ eV})$, that extends towards a higher eKE with decreasing intensity. The breadth of the feature in the PPC spectrum is consistent with DPD occurring via multiple excited states, favoring the higher energy radical state as evidenced by the higher intensity at low eKE. The energetics diagram in Figure 2 indicates that the $1^2A''$ and $2^2A'$ radical energy levels of the carboxyl isomer are energetically accessible at 4.66 eV and higher in energy than the dissociation asymptote. It is interesting to note that the decarboxylation of p-CA$^-$ is characterized by a lower peak KER and a lower branching ratio to DPD than the analogous decarboxylation of benzoate, or other previously studied carboxylates. Potentially this may be

explained by resonance stabilization of the carboxyl, resulting in a flatter dissociative potential energy surface. A calculated KE$_{max} = 0.74$ eV can be determined from the calculations detailed in section 2 and is plotted on the PPC spectrum in Figure 6b in black. The KE$_{max}$ is shifted to the high energy side of the most intense part of the spectrum, with a significant number of events appearing beyond the KE$_{max}$. This is similar to the PPC spectrum for benzoate and consistent with room temperature anions readily undergoing DPD via the $1^2A''$ radical state, but DPD only occurring for the most vibrationally excited anions via the $2^2A'$ radical state.

Previous experiments on this apparatus have indicated some vibrational excitation of the parent anions, characterized by a vibrational temperature of 298 K. At 298 K the majority of ions are in the vibrational ground state, but the Boltzmann distribution has a high energy tail, with some anions exhibiting significant vibrational excitation.[15] Previous work has demonstrated that a vibrational temperature of 298 K and the overall kinetic energy (eKE and KER) resolution of the apparatus results in a calculated KE$_{max}$ that bisects the most intense portion of the PPC spectrum, indicating that the benzoate and p-CA$^-$ spectra are consistent with a 298 K anion vibrational temperature.[15,28,33,34] The energy resolution of a PPC spectrum is 12%,[15] and therefore only events with a total energy (E$_{TOT}$ = eKE + KER) of E$_{TOT} > 0.83$ eV for p-CA$^-$ and E$_{TOT} > 1.24$ eV for benzoate can be conclusively attributed to vibrationally excited parent anions. Nonetheless the presence of some of these events, particularly for p-CA$^-$, raises the possibility that high-frequency vibrational modes are ineffectively cooled in the ion trap. This may be more pronounced in p-CA$^-$ as the greater number of degrees of freedom increase the number of high-frequency modes present. Some of these high E$_{TOT}$ events can also result from false coincidences in double photodetachment events, however at the event rate of 0.1 events per laser shot used in this study, false coincidences should contribute only 1.5% to the data.[14]

An alternative way of displaying the PPC spectrum is to plot the E$_{TOT}$ spectrum, as a histogram of the sum of the kinetic energy of the two neutral fragments and the photoelectron for each dissociative event (E$_{TOT}$=eKE + KER). Figure 7 shows the E$_{TOT}$ spectra of benzoate and p-CA$^-$ at 4.66 eV. There is a peak and an unresolved shoulder at higher energy seen in the benzoate spectrum, demonstrating the presence of low and high E$_{TOT}$ channels, attributable to decarboxylation via the B and A states of the radical respectively. The high energy tail in the benzoate E$_{TOT}$ spectrum (Figure 7) is composed of anions with substantial vibrational excitation and is associated with dissociation via the A state, as evidenced by the correlation of high E$_{TOT}$ with high eKE in the benzoate PPC spectrum in Figure 6. The majority of benzoate anions undergo dissociation upon photodetachment (90%), but only a small subset of anions undergo DPD via the A state. This is consistent with anions with the highest level of internal excitation undergoing DPD via the A state, representing the high energy tail of the vibrational Boltzmann distribution. In contrast anions with less internal excitation undergo DPD via the B state or form stable radicals following photodetachment. Similarly, the most intense portion of the p-CA$^-$ E$_{TOT}$ spectrum is
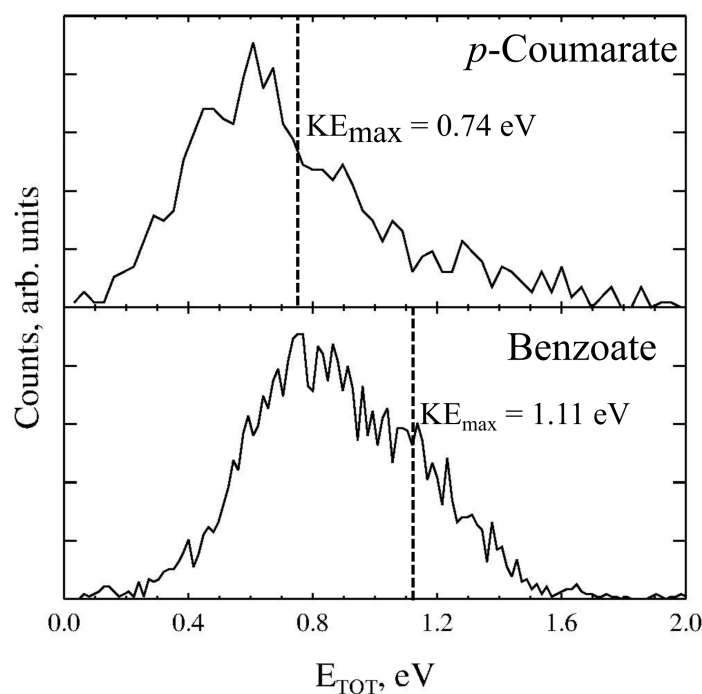
Fig. 7 The E_{TOT} spectra recorded at 266 nm (4.66 eV) for benzoate and p-CA$^-$. The KE$_{max}$ is also plotted for the decarboxylation of benzoate and p-CA$^-$.

Anion	TDE(X), eV	Peak KER eV	DPD ratio
$C_6H_5CO_2^-$	3.6	0.6	0.9
$HOC_6H_4CHCHCO_2^-$	3.6	0.45	0.1
$HO_2CCHCHC_6H_4O^-$	2.6	-	0

Table 2 The TDE to the X state of the radical, the peak KER and the branching ratio to DPD.

assignable to DPD via the $1^2A''$ radical state that occurs for room temperature anions, whereas the high energy tail is associated with DPD of vibrationally excited anions via the lower lying $2^2A'$ radical state. The high energy tail extends further from the calculated KE$_{max}$ for p-CA$^-$ than benzoate. The DPD branching ratio for p-CA$^-$ is 5%, with only a small subset of these anions undergoing DPD via the $2^2A'$ radical state, suggesting that this can only occur for the most vibrationally excited p-CA$^-$. Overall, the evidence for DPD occurring via two excited states is weaker for p-CA$^-$ than benzoate.

5 Discussion

Table 2 summarizes the findings of the PPC spectroscopy studies of the carboxylate and the phenolate form of p-CA$^-$ and benzoate at 4.66 eV. It includes the experimentally measured TDE to the radical X states as shown in Figure 4, the position of maximum intensity in the KER spectrum and the fractional branching ratio to DPD. In this discussion section the results for the three anions will be compared and contrasted.

The TDE of the carboxylate form of p-CA$^-$ and the benzoate anion are very similar, at 3.6 eV. The ground state of the carboxyl radical is stable in both cases studied here. It is difficult to extract an exact EA from the spectra presented in Figure 4 due to the vibrational excitation in the parent anions and the experimental resolution. The TDE reported here are similar to other values reported for carboxylates,[13] suggesting that the electron is photodetached from an orbital localized on the carboxylate group. The phenolate form of the p-CA$^-$ anion has a much lower TDE, near 2.6 eV, as the resulting radical is resonance

stabilized. In this case the ejected photoelectron is localized on the phenoxide group.

For benzoate and the carboxylate form of p-CA$^-$ DPD occurs from the excited states, indicating a repulsive character in the excited carboxyl states. The ground state of both carboxyl radicals are shown to be longer lived than the flight time from the interaction region to the detector ($\approx 10\mu s$). The relative energetics in Figure 2 indicate that the $C_6H_5CO_2(X)$ state is slightly higher in energy than the DPD asymptote while the p-CA carboxyl X state is the same energy as the DPD asymptote, suggesting these radical states are metastable. The DPD branching ratio is far larger for benzoate than p-CA$^-$ with over 95% of the $C_6H_5CO_2$ and approximately 10% of the $HOC_6H_4CHCHCO_2$ radical (5% of all p-CA) dissociating, assuming an equal amount of phenolate and carboxylate in the p-CA$^-$ anion beam where only the carboxylate dissociates. In both cases, the dominant dissociation channel is a two-body DPD resulting in decarboxylation, driven by the thermodynamic stability of the CO_2. The relative energetics of the dissociation asymptotes for the benzoate and the carboxylate form of p-CA$^-$ were calculated, as reported in Table 1 and Figure 2. All of the benzoate radical states were calculated to lie energetically above the $C_6H_5 + CO_2 + e^-$ asymptote, with an energy difference from the dissociative A and B states to the DPD products of 0.40 eV and 0.64 eV respectively. In contrast the first and second excited states in p-CA were calculated to be just 0.15 eV and 0.26 eV higher in energy than the $HOC_6H_4CHCH + CO_2 + e^-$ DPD asymptote. Therefore the difference in the branching ratio may be attributed to the differing stability of the aromatic radicals. No DPD of the phenolate form of p-CA$^-$ is observed, as only decarboxylation products are reported. It may be expected that dissociation of the phenolate form of p-CA would result in H or O fragments, due to the stabilization of the carbon backbone in both the anion and phenoxy radical by resonance forms.

Our results for benzoate show many similarities to the previous work of Jouvet and coworkers.[17] They observed dissociation to occur at a photon energy of 3.88 eV, which would correspond to an eKE= 0.78 eV at the 4.66 eV photon energy used here. This is similar to the high eKE onset of the feature in the benzoate PPC spectrum in Figure 6. They also observed evidence for dissociation occurring via a repulsive potential energy surface.

Various theoretical and experimental approaches were used to produce an estimate of the peak KER, ranging from 0.32 eV to 0.7 eV.[17] Unlike that previous work, our experimental method directly measures the KER spectrum, finding a peak KER of 0.6 eV. Additionally, Jouvet and coworkers reported a branching ratio to dissociation of 90% at a photon energy of 4.5 eV,[17] consistent with the branching ratio we report at 4.66 eV. In the previous study benzoate was reported to have an anion vibrational temperature of 30 K, which is lower than the room temperature anions used in this study. Finally, Jouvet and coworkers did not observe any anionic fragments despite probing for their presence directly, in agreement with our study.

For both species the calculated KE_{max} bisects to the high energy side of the most intense portion of the PPC and E_{TOT} spectra, with a tail extending to higher energies. Only events in the PPC and E_{TOT} spectra at higher energy than $E_{TOT} > 0.83$ eV for p-CA$^-$ and $E_{TOT} > 1.24$ eV for benzoate can be definitively attributed to vibrationally excited parent anions, due to the spectral energy resolution of 12%. Some of the high E_{TOT} events present may result from vibrationally excited anions, where high-frequency vibrational modes are inefficiently cooled in the ion trap, leading to a non-Boltzmann anion internal energy distribution as previously observed in the case of HOCO$^-$.[35] The most intense features in the spectra are consistent with the previously reported anion vibrational temperature of 298 K for this apparatus.[15]

The high E_{TOT} tails in the PPC and E_{TOT} spectra for benzoate and p-CA$^-$ are associated with a higher eKE but a similar KER to the low E_{TOT} feature, suggesting DPD from a lower lying radical state. This suggests that only photodetachment of the most vibrationally excited anions to the lower lying radical state results in DPD, with the remainder forming stable carboxyl radicals or undergoing DPD by a higher lying radical state. For the benzoate radical the high E_{TOT} feature is associated with the A state and it is probable that a similar low-lying excited state, probably the $2^2A'$ state, is responsible for the high energy tail in p-CA$^-$. These electronic state assignments are determined from the previously reported energetics of the carboxylate form of p-CA.[25] The most intense features in both spectra have lower E_{TOT} than the expected upper limit to the E_{TOT} spectrum, the calculated KE_{max}, and are associated with DPD occurring via the second excited radical state. As the second excited radical state lies higher in energy than the dissociation asymptote, DPD can occur without vibrational promotion. For benzoate and p-CA$^-$ this occurs from the B and $1^2A''$ radical states respectively. This effect is amplified for p-CA$^-$ where the high energy tail in the E_{TOT} spectrum is shifted to higher energies relative to KE_{max} than the benzoate spectrum. For p-CA$^-$ only 5% of anions undergo DPD, and only a small fraction of these anions undergo DPD via the $1^2A''$ state, suggesting that these anions are the hottest anions in the ion beam, forming the high energy tail of the anion internal energy distribution.

Both benzoate and p-CA$^-$ have planar anion structures as a result of the conjugation between the aromatic ring and the carboxylate group, which in the latter case are linked by a carbon-carbon double bond. The planar structure places a barrier to free rotation of the CO_2 relative to the ring, as rotation out of plane will result in reduced overlap between neighboring π systems and the loss of stabilization of the anion due to resonance effects. Previous photoelectron spectroscopy measurements and corresponding calculations have indicated a 19° change in the OCO bond angle upon photodetachment of benzoate to the corresponding planar neutral, and resolved vibrational structure.[16] This indicates that upon photodetachment the CO_2 bending mode will be excited, and DPD would therefore result in a vibrationally excited CO_2 molecule. If an anion in the vibrational ground state undergoes DPD to form vibrationally excited products, then the E_{TOT} will be lower than the calculated KE_{max}, by the amount of internal excitation in the products. The substantial width of the most intense portions of the benzoate and p-CA$^-$ PPC and E_{TOT} spectra indicate the presence of substantial vibrational excitation in the products, likely in the CO_2 fragment.

The calculated energetics reported in Table 1 indicate that two-body ionic photodissociation channels are energetically accessible for both p-CA$^-$ and benzoate at 4.66 eV. Two three-body photodissociation channels for p-CA$^-$ are calculated to be energetically accessible as well. It is challenging to directly probe photodissociation using one-photon PPC spectroscopy, as ionic fragments are not detected. However, experimental evidence is seen for the three-body photodissociation of p-CA$^-$ ($HOC_6H_4CHCHCO_2^- \xrightarrow{h\nu} HOC_6H_5 + HCC^- + CO_2$) in the fragment mass spectrum (SI Figure S4). This product channel requires H atom transfer to occur from the $\alpha-C$ to the aromatic ring in concert with the three-body photodissociation. This photodissociation would be driven by the thermodynamic stability of CO_2 and C_6H_5OH.

6 Conclusions

We employed PPC spectroscopy to study the photodetachment and DPD of benzoate and p-CA$^-$ at 4.66 eV. We also calculated the relative energetics of the photodissociation and DPD channels of p-CA$^-$ and benzoate. The results show that photodetachment of $C_6H_5CO_2^-$ results predominantly in $CO_2 + C_6H_5 + e^-$ via a two-body DPD process, with a minor channel resulting in the formation of stable $C_6H_5CO_2$. Our results indicate that the X state is stable, whereas the A and B states are dissociative. The phenolate and carboxylate isomers of p-CA$^-$ are both observed. Upon photodetachment of the phenolate isomer of p-CA$^-$ stable radicals result, whereas in addition to forming stable radicals a small portion of the carboxylate isomer undergoes two-body DPD resulting in $CO_2 + HOC_6H_4CHCH$ and three-body photodissociation resulting in $CO_2 + HCC^- + HOC_6H_5$. Both carboxylate anions exhibit metastable ground states and undergo decarboxylation from multiple excited states, with DPD occurring only for the vibrationally hottest anions in the ion beam from the lower energy radical excited states. In the future these studies will be extended to other complex carboxylates of importance in biology.

Conflicts of interest

AIK is the president and part-owner of Q-Chem, Inc.

Acknowledgements

Notes and references

1 T. Meyer, Biochimica et Biophysica Acta (BBA) - Bioenergetics, 1985, **806**, 175 – 183.

2 C. R. S. Mooney, M. A. Parkes, A. Iskra and H. H. Fielding, Angewandte Chemie International Edition, 2015, **54**, 5646–5649.

3 I.-R. Lee, W. Lee and A. H. Zewail, Proceedings of the National Academy of Sciences, 2006, **103**, 258–262.

4 A. Henley, A. M. Patel, M. A. Parkes, J. C. Anderson and H. H. Fielding, The Journal of Physical Chemistry A, 2018, **122**, 8222–8228.

5 M. A. Parkes, C. Phillips, M. J. Porter and H. H. Fielding, Phys. Chem. Chem. Phys., 2016, **18**, 10329–10336.

6 A. Henley, M. E. Diveky, A. M. Patel, M. A. Parkes, J. C. Anderson and H. H. Fielding, Phys. Chem. Chem. Phys., 2017, **19**, 31572–31580.

7 I. B. Nielsen, S. Boyé-Péronne, M. O. A. El Ghazaly, M. B. Kristensen, S. Brøndsted Nielsen and L. H. Andersen, Biophysical Journal, 2005, **89**, 2597–2604.

8 L. Lammich, J. Rajput and L. H. Andersen, Phys. Rev. E, 2008, **78**, 051916.

9 T. Rocha-Rinza, O. Christiansen, J. Rajput, A. Gopalan, D. B. Rahbek, L. H. Andersen, A. V. Bochenkova, A. A. Granovsky, K. B. Bravaya, A. V. Nemukhin, K. L. Christiansen and M. B. Nielsen, The Journal of Physical Chemistry A, 2009, **113**, 9442–9449.

10 T. Rocha-Rinza, O. Christiansen, D. B. Rahbek, B. Klærke, L. H. Andersen, K. Lincke and M. B. Nielsen, Chemistry A European Journal, 2010, **16**, 11977–11984.

11 L. H. Andersen, A. V. Bochenkova, J. Houmøller, H. V. Kiefer, E. Lattouf and M. H. Stockett, Phys. Chem. Chem. Phys., 2016, **18**, 9909–9913.

12 J. N. Bull, G. d. Silva, M. S. Scholz, E. Carrascosa and E. J. Bieske, The Journal of Physical Chemistry A, 2019, **123**, 4419–4430.

13 J. A. Gibbard and R. E. Continetti, In preparation, 2020.

14 R. E. Continetti, International Reviews in Physical Chemistry, 1998, **17**, 227–260.

15 J. A. Gibbard, A. J. Shin, E. Castracane and R. E. Continetti, Review of Scientific Instruments, 2018, **89**, 123304.

16 H.-K. Woo, X.-B. Wang, B. Kiran and L.-S. Wang, The Journal of Physical Chemistry A, 2005, **109**, 11395–11400.

17 G. A. Pino, R. A. Jara-Toro, J. P. Aranguren-Abrate, C. Dedonder-Lardeux and C. Jouvet, Phys. Chem. Chem. Phys., 2019, **21**, 1797–1804.

18 R. F. Gunion, M. K. Gilles, M. L. Polak and W. Lineberger, International Journal of Mass Spectrometry and Ion Processes, 1992, **117**, 601 – 620.

19 M. Almasian, J. Grzetic, J. van Maurik, J. D. Steill, G. Berden, S. Ingemann, W. J. Buma and J. Oomens, The Journal of Physical Chemistry Letters, 2012, **3**, 2259–2263.

20 D. Zuev, K. B. Bravaya, M. V. Makarova and A. I. Krylov, The Journal of Chemical Physics, 2011, **135**, 194304.

21 K. B. Bravaya, M. G. Khrenova, B. L. Grigorenko, A. V. Nemukhin and A. I. Krylov, The Journal of Physical Chemistry B, 2011, **115**, 8296–8303.

22 E. Epifanovsky, I. Polyakov, B. Grigorenko, A. Nemukhin and A. I. Krylov, Journal of Chemical Theory and Computation, 2009, **5**, 1895–1906.

23 K. B. Bravaya and A. I. Krylov, The Journal of Physical Chemistry A, 2013, **117**, 11815–11822.

24 S. H. M. Deng, X.-Y. Kong, G. Zhang, Y. Yang, W.-J. Zheng, Z.-R. Sun, D.-Q. Zhang and X.-B. Wang, The Journal of Physical Chemistry Letters, 2014, **5**, 2155–2159.

25 D. Zuev, K. B. Bravaya, T. D. Crawford, R. Lindh and A. I. Krylov, The Journal of Chemical Physics, 2011, **134**, 034310.

26 K. Bhaskaran-Nair, M. Valiev, S. H. M. Deng, W. A. Shelton, K. Kowalski and X.-B. Wang, The Journal of Chemical Physics, 2015, **143**, 224301.

27 Z. Lu and R. E. Continetti, The Journal of Physical Chemistry A, 2004, **108**, 9962–9969.

28 J. A. Gibbard, E. Castracane, A. J. Shin and R. E. Continetti, Phys. Chem. Chem. Phys., 2020, **22**, 1427–1436.

29 M. S. Bowen and R. E. Continetti, The Journal of Physical Chemistry A, 2004, **108**, 7827–7831.

30 D. P. de Bruijn and J. Los, Review of Scientific Instruments, 1982, **53**, 1020–1026.

31 P. Pokhilko, E. Epifanovskii and A. I. Krylov, J. Chem. Theory Comput., 2018, **14**, 4088–4096.

32 Y. Shao et al, Molecular Physics, 2015, **113**, 184–215.

33 J. A. Gibbard and R. E. Continetti, Molecular Physics, 2019, **117**, 3056–3065.

34 J. A. Gibbard and R. E. Continetti, Faraday Discussions, 2019, **217**, 203–219.

35 C. J. Johnson, R. Otto and R. E. Continetti, Phys. Chem. Chem. Phys., 2014, **16**, 19091–19105.